CHAPTER 2

Synthesis of α-Fe$_2$O$_3$ nanopowder by using PVA precursor based method

2.1 Experimental Procedure for Chemical Synthesis:

The starting chemicals used were ferric nitrate nonahydrate (99.9%, Merck, India), PVA (polyvinyl alcohol) of mol. wt. 1, 25,000 (99.9%, Merck, India) and sucrose (99.9%, Merck, India) without further purification.

Aqueous solutions of PVA (10 wt %) and ferric nitrate were mixed vigorously in a molar ratio of 2.5:1 by using a magnetic stirrer. An aqueous solution of sucrose (10-wt% of sucrose with respect to PVA) was added to this mixture and stirred for 1hour at room temperature. A dark brown colored fluffy precursor was formed when this mixture was dried on a hot plate at ~125^{0}C.

Pure α-Fe$_2$O$_3$ nanopowder was obtained by calcining the precursor powder for two and a half hours at different temperatures ranging from 250 to 450^{0}C in air [123, 124]. In order to avoid contamination of the precursor by carbon, a few drops of saturated ammonium nitrate solution was added to the precursor powders during the time of calcination.

2.2 Results and Discussion:

2.2.1 Thermal Analysis:

TG-DTG (Differential Thermogravimetric) and DSC analyses were performed to investigate the decomposition behavior of the precursor powders due to heat treatment in air and thermograms are shown in Fig 2.1.
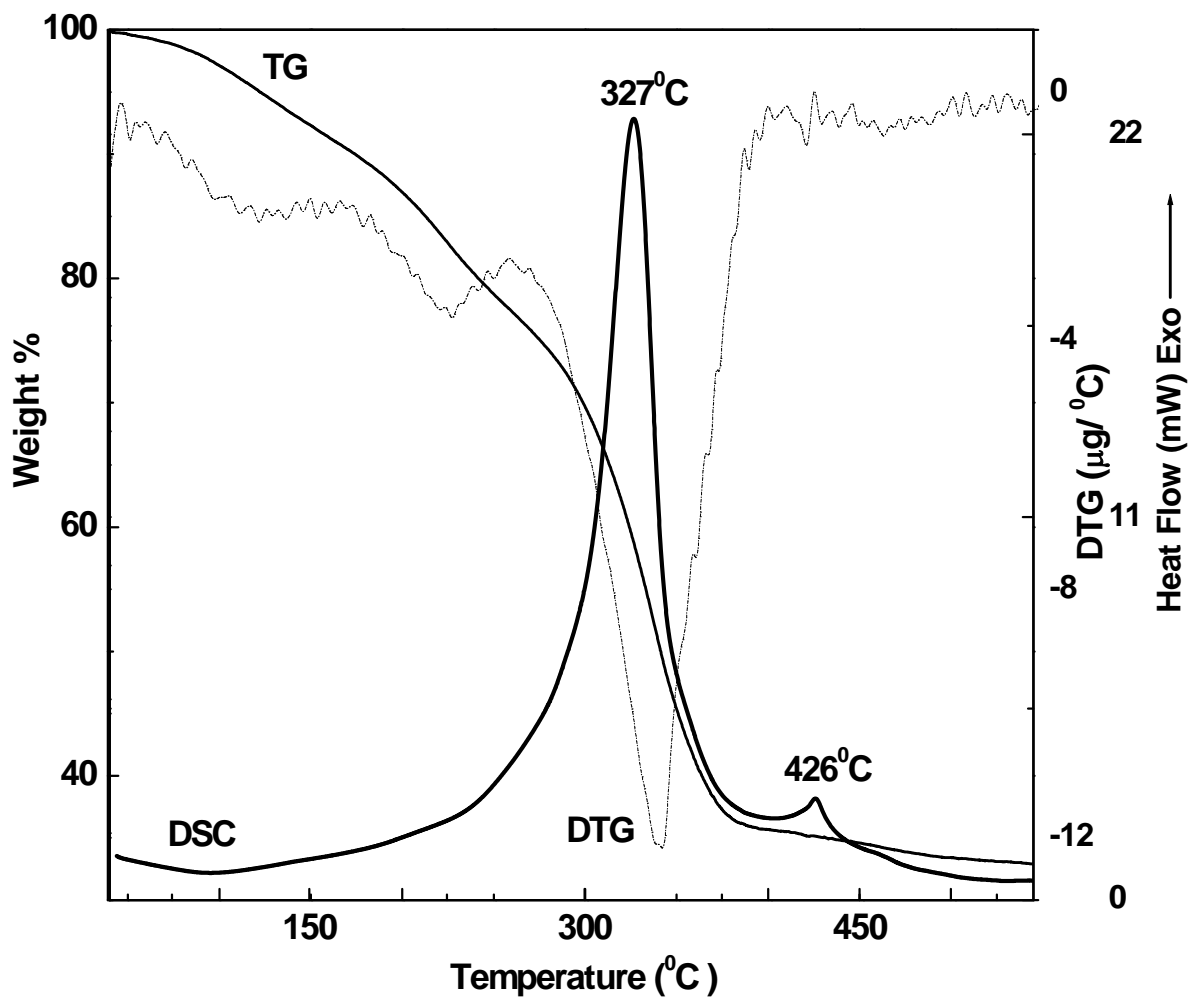
Fig 2.1 TG-DTG and DSC thermograms of the precursor in air.

The important features of the thermograms are as follows:

(i) In TG thermogram, a total weight loss of ~65% was observed.

(ii) Weight loss of ~14% occurred from 40-200^{0}C. This weight loss was due to loss of moisture from the precursor followed by the removal of strongly adsorbed water molecules.

(ii) Major weight loss of 51% occurred in the region from 200 to 450^{0}C and this weight loss was attributed to the oxidative decomposition of the organic components of the precursor leading to the evolution of NO_x and CO_2 gases. This decomposition was reflected in DSC thermogram as exothermic peaks at 327 and 426^{0}C.

(iv) Heating the sample beyond 460^{0}C resulted in neither a weight loss nor formation of any new peak in the thermograms. This confirmed the full decomposition of the precursor to iron oxide at ~460^{0}C [123, 124].

2.2.2 X-Ray Analysis:

Room temperature XRD spectra of powders calcined at different temperatures are shown in Fig. 2.2 (a) and (b). The main features of the spectra are as follows:

(i) It was observed that the precursor was completely amorphous.

(ii) The appearance of two main intensity peaks corresponding to (104) and (110) diffraction planes for powder calcined at 250^{0}C, indicated the beginning of the formation of α-Fe₂O₃ phase.

(iii) Complete formation of single phase α-Fe₂O₃ occurred when precursor was calcined at 450^{0}C for two and a half hours in air [123, 124].

(iv) Appearance of diffraction peaks at 2θ = 24.4^0, 33.3^0, 35.8^0, 41.0^0, 49.5^0, 54.3^0, 57.7^0, 62.6^0, and 64.2^0 were in good agreement with the corresponding (012), (104), (110), (113), (024), (116), (018), (214) and (300) diffraction planes of α-Fe₂O₃ respectively (JCPDS 80-2377).

(v) Slow scan of the two main intensity peaks was performed and crystallite size of powders calcined at different temperatures was calculated using Scherrer's equation [125]. They lie in the range of 25-30 nm depending upon the calcination temperature.
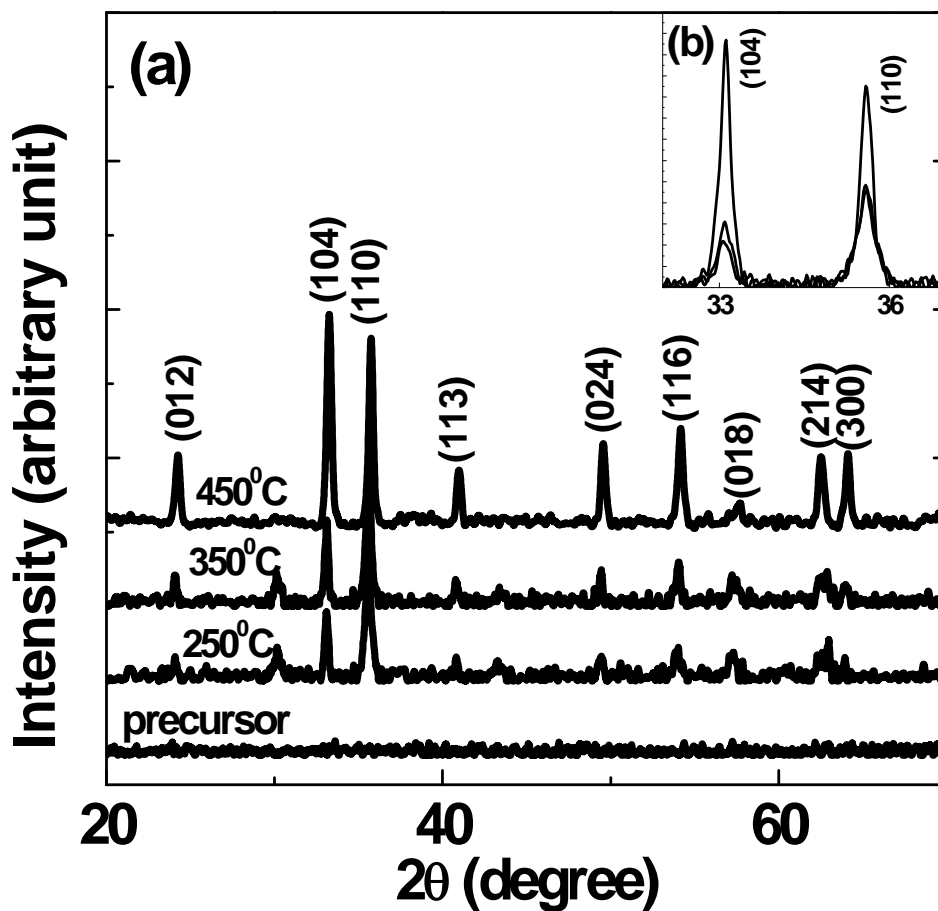
Fig 2.2 (a) X-ray diffraction spectra of precursor powder at different calcination temperatures (b) slow scan of the (104) and (110) diffraction planes.

2.2.3 TEM Analysis:

TEM micrograph of the precursor powder calcined at 450^0C is shown in Fig. 2.3. It clearly indicated that average particle size of the calcined powder was ~30 nm and it matched well with that calculated by XRD analysis. The particles were mostly elongated in shape and formed loose aggregates.
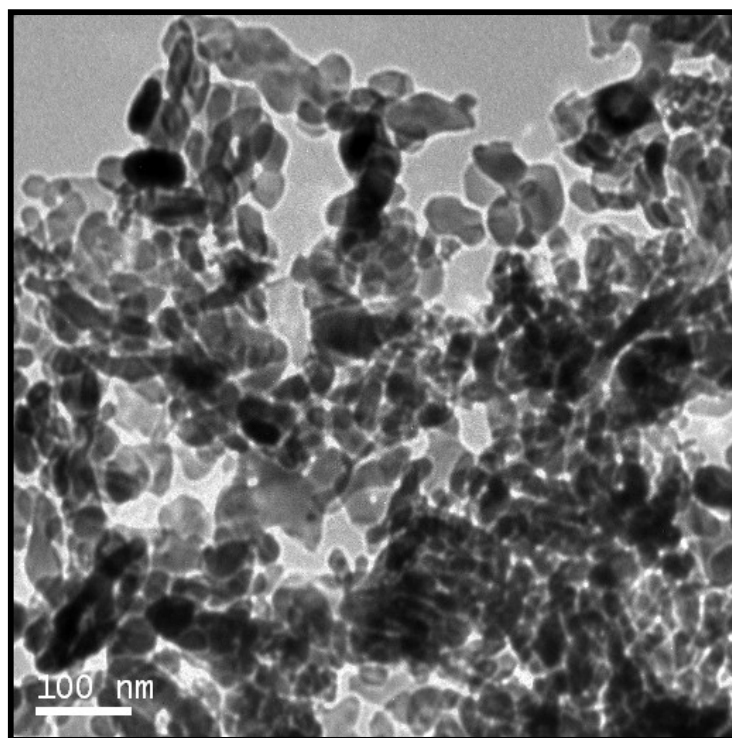

Fig 2.3 TEM micrograph of α-Fe₂O₃ powder calcined at 450^0C.

2.2.4 SEM Analysis:

The SEM study was performed by preparing two kinds of samples. One sample was the calcined precursor that constituted of nanosized grains and the other was obtained by sintering the as-obtained nanopowder at a temperature of 1100^0C for 2 hours. The SEM micrographs are shown in Fig. 2.4(a) and (b).
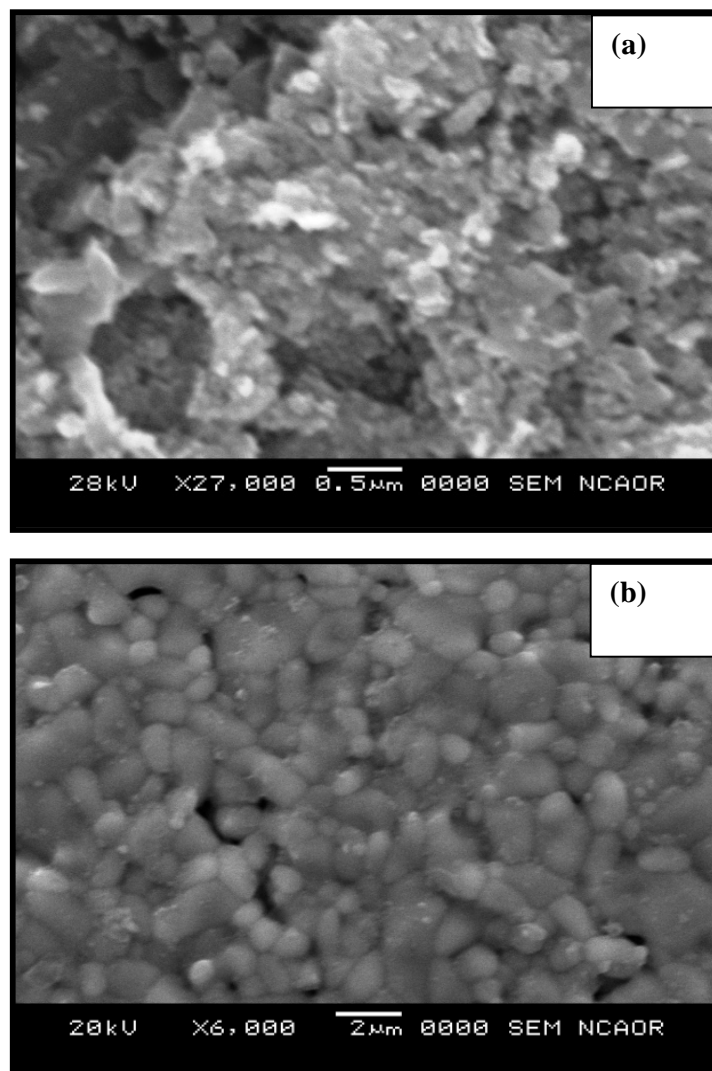

Fig. 2.4 SEM micrographs of α-Fe$_2$O$_3$ powder (a) calcined at 450^0C and (b) sintered at 1100^0C.

The micrographs exhibited the following features:

(i) The calcined sample showed loose aggregation of nanoparticles and formation of voids.

(ii) The pellets sintered at high temperature revealed a uniform microstructure of the coarsened grains. Coarsening of grains at elevated temperature was observed due to fusion of the nanosize particles. As a result, the grain size was in the micrometer range for the sintered samples.

(iii) The particles in both cases were found to be elongated and the shape of particles was in *sync* with the hexagonal corundum structure of α-Fe₂O₃ [1].

2.2.5 DC resistivity measurement:

The variation of DC resistivity with change in temperature was studied for two cases (i) unsintered pellet and (ii) pellet sintered at 1100^0C for 2 hours and these are shown in Fig. 2.5(a) and (b). Room temperature recorded was 28^0C. The green density and sintered density of the pellets was calculated by using the dimensions of the pellets.

Case (i) unsintered pellet:

DC resistivity of the unsintered sample increased slowly with increase in temperature, attained a maximum and then decreased with further increase in temperature. As was seen in SEM micrograph (Fig. 2.4(a)), the microstructure of the unsintered sample consisted of loosely agglomerated particles with high intergranular porosity (green density was ~ 2.4 g/cm^3). The adsorption of moisture in the nanopores (humidity recorded in our lab was ~91% at room temperature) and the subsequent elimination of moisture at ~100^0C gave rise to the maximum in the resistivity [12, 13, 123, 124, 126]. Beyond ~100^0C, when all moisture was eliminated, the curves exhibited the typical NTCR (negative temperature coefficient of resistance) behavior of bulk hematite [127].

Case (ii) pellet sintered at 1100^0C:

On sintering, the nanosized sample not only grew to micron size but there was densification of the sample as well. Sintered density attained by the sample was ~ 4.8 g/cm^3. The adsorption of moisture was less prominent as there was fewer numbers of pores. Therefore, the adsorption of moisture or its elimination for the sintered sample was not reflected anywhere in the curve (Fig. 2.5(b)) and the behavior was NTCR throughout the temperature
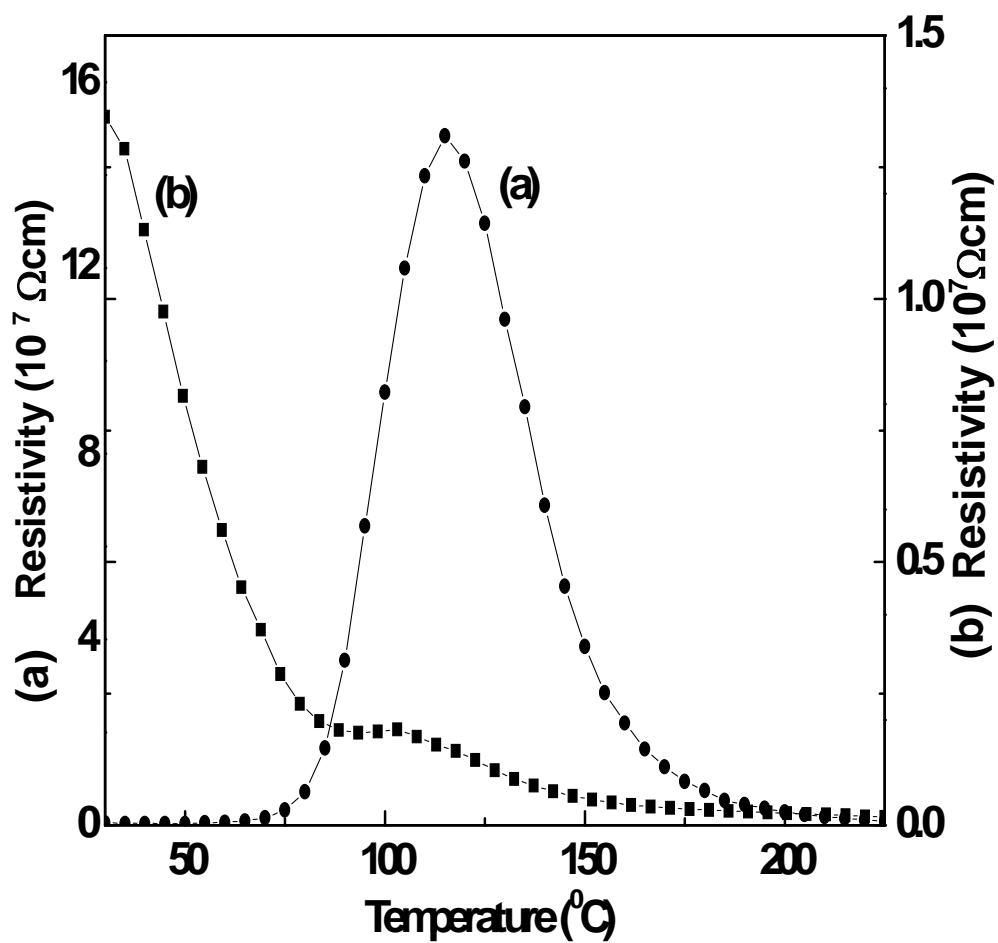
Fig. 2.5. Variation of DC resistivity with change in temperature of α-Fe$_2$O$_3$ powder for (a) unsintered sample (b) sample sintered at 1100^0C.

range. This inference was supported by the respective SEM micrograph (Fig. 2.4(b)) where large grains and a densified microstructure were observed.

Discussion:

TG-DTG-DSC, XRD and TEM analyses of the synthesized precursors and calcined powders confirmed that oxidative decomposition of precursor leads to the formation of single phase α-Fe_2O_3 nanopowders. The chemical process starts from homogeneous distribution of metal ions in solution. Sucrose serves as a chelating agent and ensures that water-soluble iron ions are uniformly anchored in the polymeric network structure of PVA. This possibly serves to prevent their segregation or any intermittent precipitation from the homogeneous precursor solution during evaporation. A fluffy mass forms due to complete evaporation of the solution, which is effectively a carbonaceous material having a porous structure. During decomposition of these iron ion-containing precursors, nascent iron oxide forms, which are small atomic clusters with proper chemical homogeneity, imbedded in this porous carbonaceous material. This nascent iron oxide finally produces desired single-phase α-Fe_2O_3 nanopowders. The decomposition of carbonaceous material produces gases (such as CO, CO_2, NO_X and water vapor) that help the precursor material to dissipate the heat of combustion and thus inhibit the sintering of fine particles during the process to produce nanosized iron oxide [57, 123].

SEM micrographs and DC resistivity measurements indicated that the resistivity behavior of the synthesized nanopowders with respect to temperature was affected by the presence of moisture in the air due to large amount of porosity in the samples. The resistivity behavior of the sintered sample was independent of the presence of moisture. This can be attributed to the density achieved on sintering the nanoparticles which was close to bulk density of 5.24 g/cm^3 [128]. This indicates a correlation between the microstructure and DC resistivity measurement for the powder synthesized by PVA precursor based method.

2.3 Summary of Results:

1. α-Fe_2O_3 nanopowder was successfully synthesized by using PVA precursor based synthesis route.

2. Thermal decomposition of the precursor was complete at ~460^{0}C.

3. Single phase α-Fe_2O_3 nanopowder was synthesized at a calcination temperature of 450^{0}C for two and a half hours in air.

4. Average particle size of the nanopowder was ~30 nm.

5. Surface morphology studies revealed that the particles were elongated in shape for nanopowders as well as samples sintered at 1100^0C.

6. Room temperature resistivity of as-synthesized nanopowder was ~10^5 Ω cm.